5 January 2001

ELSEVIER

Chemical Physics Letters 333 (2001) 76–82

CHEMICAL PHYSICS LETTERS

www.elsevier.nl/locate/cplett

Femtosecond photon echo and virtual echo measurements of the vibronic and vibrational coherence relaxation times of iodine vapor

Igor Pastirk [a,1], Vadim V. Lozovoy [a,2], Marcos Dantus [a,*]

[a] *Department of Chemistry and Center for Fundamental Materials Research, Michigan State University, East Lansing, MI 48824-1322, USA*

Received 9 October 2000; in final form 6 November 2000

Abstract

Femtosecond three-pulse four-wave mixing (FWM) techniques are used to sort and measure the processes that contribute to coherence relaxation. We compare the observed relaxation times for vibronic coherence using photon echo (PE) and reverse transient grating (RTG) measurements at different temperatures to isolate inhomogeneous and homogeneous components. Different pulse sequences are used to select ground or excited state vibrational coherences. Measurements of ground and excited state wave packet spreading times due to anharmonicity, a process that does not involve energy dissipation or phase relaxation, are also presented.

1. Introduction

The loss of quantum mechanical coherence, a T_2 process, in gas phase samples is caused by collisions and inhomogeneous broadening (for example Doppler broadening). The cross-section of these processes depends on the type of coherence. In a molecular system, one can identify electronic, vibrational and rotational coherences. Vibrational and rotational coherences can be found in a selected electronic state (ground or excited), and electronic coherences can include rotational and vibrational components as well. In the present study, three-pulse four-wave mixing (FWM) techniques are applied to experimentally measure the homogeneous, T_2', and inhomogeneous, T_2^*, vibronic coherence relaxation times of iodine vapor.

Starting with the first observation of photon echo (PE) in the condensed and gas phase [1,2], it was clear that this non-linear optical method, analogous to spin echo techniques in NMR [3], was capable of providing coherence relaxation measurements free of inhomogeneous broadening. In the last decade, these measurements have been combined with ultrafast lasers to measure coherence relaxation times in large organic molecules in solution [4–6]. This method has not been as popular for the study of gas phase samples. Here we illustrate its advantages.

* Corresponding author. Fax: +1-517-353-1793.
E-mail address: dantus@msu.edu (M. Dantus).
[1] Affiliated with the Institute for Nuclear Sciences, VINCA, Belgrade, Yugoslavia
[2] Permanent address: N.N. Semenov Institute of Chemical Physics, RAS, Moscow, Russia.

0009-2614/01/$ - see front matter
PII: S0009-2614(00)01334-8

There are many studies on the relaxation time of iodine in the gas phase. Among them are measurements of T_1 relaxation (loss of population in the excited state) due to self-quenching [7,8], cross-section measurements of phase relaxation in the presence of noble gases with femtosecond pump–probe methods [9,10] and T_2 measurements by PE techniques in the nanosecond timescale [11]. The goal of our measurements is to determine the rate of vibrational coherence relaxation of the excited (B) and ground (X) states independently as well as the homogeneous and inhomogeneous vibronic coherence involving the two electronic states.

The theoretical foundation of these measurements is best expressed in terms of the time evolution of the density matrix in Liouville space [12,13]. A more detailed description of this theory as it applies to our measurements has been published elsewhere [14,15]. The density matrix of a multilevel system involving several vibrational levels in the ground and excited states, indicated by indices e and g, can be divided into four blocks. In the diagonal blocks, the elements (gg or ee) represent the populations of each vibrational level. Within the diagonal block, off-diagonal elements ($g'g$, gg' or $e'e$, ee') represent vibrational coherence. The elements of the off-diagonal blocks (eg or ge) represent the vibronic coherence involving vibrational levels from both electronic states. In the presence of collisions, two types of relaxation can be observed: T_1 processes, which involve the loss of amplitude in the population terms ρ_{ii}, and T_2' processes, which involve the loss of amplitude in the coherence terms ρ_{ij}. Inhomogeneous broadening, T_2^*, does not depend on collisions but also leads to a loss of coherence. Wave packet spreading due to anharmonicity does not involve coherence relaxation, but it leads to dephasing (and rephasing) of the observed vibrational coherence, which depends on the terms $\rho_{gg'}$ and $\rho_{ee'}$. Here we define this intramolecular dephasing time as a T_3 process.

In this Letter, we present a set of measurements using three-pulse FWM techniques that can be used to sort out all the contributions to quantum mechanical coherence dephasing in a molecular gas. Four different pulse sequences are used to sort out the different relaxation processes involving the $(X)^1\Sigma_g^+$ and $(B)^3\Pi_{0u}^+$ states of molecular iodine. Homogeneous vibronic coherence relaxation between the ground and the excited states were measured using the PE pulse sequence [13,15]. The full vibronic coherence lifetime was measured with the reverse transient grating (RTG) pulse sequence [16]. The vibrational coherence relaxation in each electronic state was measured with virtual echo (VE) pulse sequences. For this method, the timing between the first two pulses was used to separate the contributions from the ground and excited states [17]. A brief discussion is included to place our findings within the perspective of relaxation measurements in molecular iodine as well as other gas phase samples.

2. Experimental

The experimental setup used to carry out the measurements has been described elsewhere [14,15]. Briefly, 60 fs transform-limited pulses (FWHM) centered at 620 nm were used. The output was split into three separate arms with $\sim$20 μJ per pulse, and were combined non-collinearly in a phase matching geometry [17–19]. The pulses were focused into a 45 mm long quartz cell. Temperature dependence was measured for PE and RTG in a cell that maintained a saturated iodine vapor pressure. The rest of the measurements were made at 200°C in a different cell where the optical density was kept constant at $\sim$0.3, a value that is well below the saturated vapor pressure. The two diagonally opposed beams (***a*** and ***c***) and the beam between them (***b***) define the phase-matched emission in the direction $\mathbf{k}_s = \mathbf{k}_a - \mathbf{k}_b + \mathbf{k}_c$ [15,16]. This arrangement predetermines the sign for each wave vector. The time ordering of each pulse (the pulse sequence) is changed for each experiment using optical delay lines. The homodyne detected signal was time (10 ns) and spectrally (16 nm) integrated. For all the pulse sequences, indicated at the top of each figure, the laser intensities were kept constant. The measurements presented here were taken with the same setup and under similar conditions. The only change was in the pulse sequence that selects the process to be measured.

3. Results and discussion

Homogeneous vibronic coherence relaxation measurements of molecular iodine as a function of temperature using the PE sequence are presented in Fig. 1a. The first pulse in the sequence generates the vibronic coherence (ρ_{ge}, and its dephasing is measured as a function of the time delay τ. The double-sided Feynman diagrams (DSFDs) are presented to indicate the non-linear process involved [13,15]. In the range from 77°C to 108°C, the signal intensity decays exponentially. Because the signal is homodyne detected, it is proportional to the square of the polarization. Hence, we use $T_2 = 2\tau_{\exp}$ to calculate the homogeneous relaxation times measured, ranging from $T'_{2eg} = 1304$ to 310 ps for the lowest and the highest temperatures (see Fig. 1a). In this temperature range, the vapor pressure increases exponentially with temperature [20]. Homogeneous relaxation is caused by collisions, therefore, it is proportional to the iodine concentration in this temperature range, $1/T'_{2eg} = n \cdot \sigma \cdot \upsilon$, where υ is the average molecular velocity, n the number density and σ is the phenomenological cross-section. Numerical calculation of the homogenous cross-section based on the experimental data gives $\sigma = 1150 \pm 150$ Å^2. This implies that long-range interactions are responsible for the collision-induced homogeneous vibronic relaxation. Our value for the homogeneous

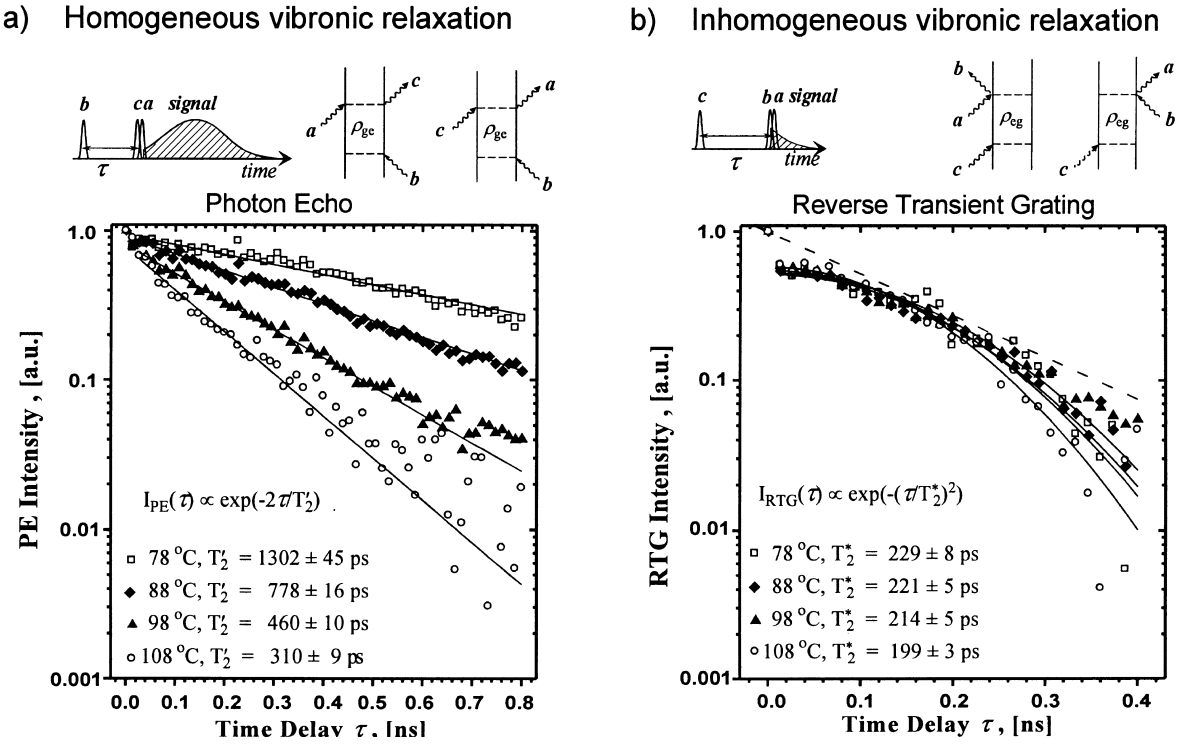

Fig. 1. (a) Pulse sequence, corresponding DSFD, and PE measurements of the homogeneous vibronic relaxation between the X and B electronic states of I_2. The time delay between the pulses ***b*** and ***a***(***c***) was scanned. The DSFD indicates that signal depends on the off-diagonal terms ρ_{ge}. The logarithm of the amplitude normalized FWM emission is plotted as a function of time delay τ. The solid lines are exponential fits to the experimental data obtained at different temperatures. (b) Pulse sequence, corresponding DSFD, and RTG measurements of the inhomogeneous vibronic relaxation between the X and B electronic states of I_2. The time delay between the pulses ***c*** and ***a***(***b***) was scanned. The DSFD shows that signal depends on the off-diagonal terms ρ_{eg}. The logarithm of the amplitude normalized signal FWM emission is plotted as a function of time delay τ. The solid lines are fits to a Gaussian function of the data obtained at different temperatures. The dashed line corresponds to the exponential decay measured for the PE data at 108°C (in (a)).

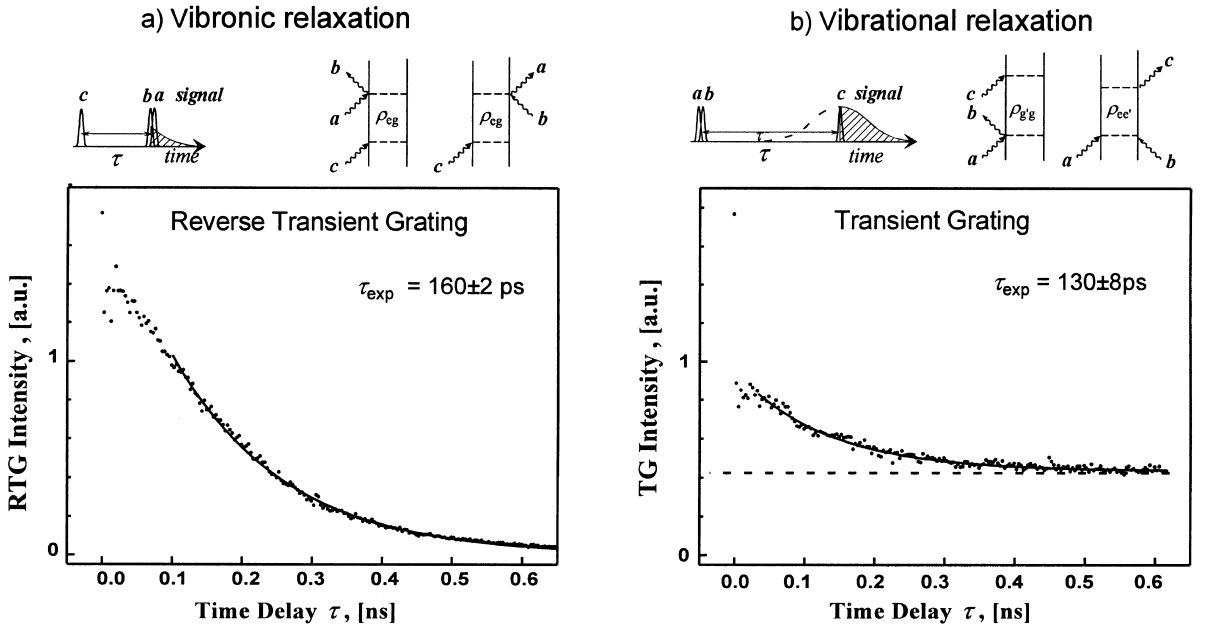

Fig. 2. (a) RTG measurements of the vibronic relaxation between the X and B electronic states of I_2. The FWM emission is plotted as a function of time delay τ. The solid line is an exponential fit to the experimental data (dots). (b) The pulse sequence and corresponding DSFD for TG measurements of vibrational coherence in the X and B electronic states of I_2. The DSFD shows that the signal depends on the elements in the diagonal blocks ρ_{gg}, $\rho_{gg'}$, $\rho_{ee'}$ and $\rho_{ee'}$. The FWM emission is shown as a function of time delay τ. The solid line is an exponential fit to the experimental data (dots). Dashed line indicates the long-lived component of this signal, which decays with T_1. The data in (a) and (b) were obtained in a special cell at 200°C (see text), and include inhomogeneous and homogenous broadening.

vibronic dephasing cross-section is larger than the vibrational dephasing cross-section measurements by Zewail's research group in the presence of noble gases [10,11]. This is to be expected when comparing self-quenching of iodine molecules to quenching by noble gas atoms such as helium, neon and argon [10,21]. The cross-section for coherence relaxation is also larger than those for T_1 relaxation due to self-quenching [7,8] as expected.

When the RTG pulse sequence is used, see Fig. 1b top, the vibronic coherence relaxation measurements include both homogeneous and inhomogeneous contributions. The experiments were carried out under the same conditions as the PE experiments. In this case, however, the data no longer follow an exponential decay. Inhomogeneous broadening gives rise to a Gaussian line shape in the frequency domain and hence in the time domain. The data in Fig. 1b were fit with the formula $S = Ae^{-(t/T_2^*)^2}$, where A is an adjustable amplitude [22]. The experimental relaxation times, in the temperature range from 77°C to 108°C, go from $T_{2eg}^* = 229 \pm 8$ to 199 ± 3 ps (see Fig. 1b). Notice that there is only a 13% difference in the relaxation rate, although, the number density increased from 3×10^{23} to 1.7×10^{24} m^{-3}. In Fig. 1b, we have included the exponential decay used to fit the PE data at 108°C. Notice that after the first 200 ps, inhomogeneous is faster than the homogeneous relaxation. The weak dependence on number density and the Gaussian decay pattern indicate that inhomogeneous contributions play a very important role in RTG measurements. Inhomogeneous contributions include Doppler broadening. Using formulas from Siegman [22]

$$\Delta\omega_D = \sqrt{\frac{(8\ln 2)kT}{Mc^2}}\omega \quad \text{and} \quad T_2^* = \frac{\sqrt{4\pi \ln 2}}{\Delta\omega_D},$$

where $\Delta\omega_D$ is the FWHM linewidth of the Gaussian distribution, M the molecular weight and ω is the central frequency of the transition, we calculate $T_2^* = 1.1$ ns for $T = 381$ K. The value

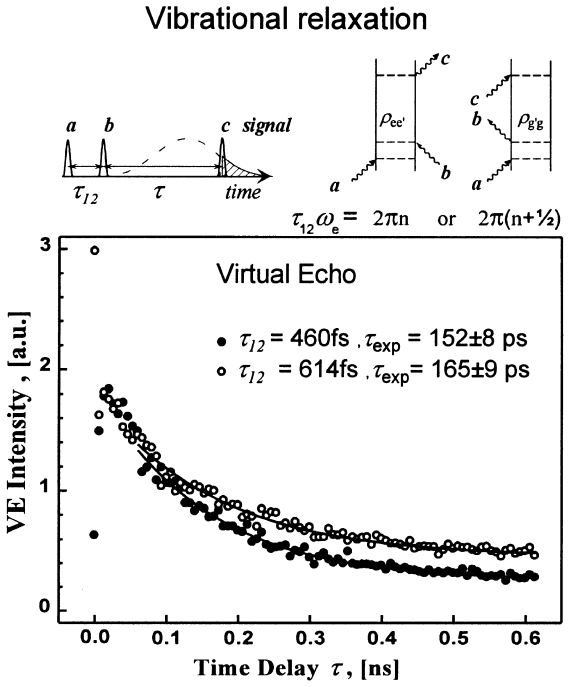

Fig. 3. (a) The sequence and corresponding DSFD for the VE pulse sequences. The DSFD show that signal depends on the $\rho_{ee'}$ and $\rho_{g'g}$ elements. (b) VE measurements of vibrational coherence in the B ($\tau_{12} = 460$ fs) and X ($\tau_{12} = 614$ fs) electronic states of I_2. The intensity of FWM emission is shown as a function of time delay τ. The solid line is an exponential fit to the experimental data (dots). The data were obtained in a special cell at 200°C (see text).

measured is of the same order of magnitude but is five times shorter. One reason for this discrepancy is that the RTG data contain both homogeneous and inhomogeneous relaxations. This explains why the measured rates exceed the expected $T^{1/2}$ dependence for inhomogeneous decay.

For PE and RTG measurements, the signal drops to 0 for long time delays. In Fig. 2a, we have included an RTG measurement obtained with a cell kept at 200°C with a low number density of iodine molecules (see Section 2). The signal approaches 0 at long times with an exponential decay time of 160 ps. For vibrational relaxation measurements, the transient grating (TG) and VE sequences were used. In both cases, the signals include the diagonal density matrix elements ρ_{ee} and/or ρ_{gg}, which relax with T_1 lifetimes. Under the experimental conditions, T_1 is very long and is manifested experimentally as a constant signal level at long times (see Fig. 2b). The exponential decay has lifetime $\tau_{exp} = 130$ ps. The time-dependent component of the TG signal includes both $\rho_{e'e}$ and $\rho_{gg'}$ vibrational coherence.

In order to separate the ground and excited state contributions to the signal we used the VE pulse sequences as described by Brown et al. [17] (see Fig. 3 on top). When the delay between first two pulses τ_{12} was 460 fs, we measured a coherence lifetime corresponding to the excited state of $\tau_{exp} = 152$ ps. When the delay τ_{12} was 614 fs the lifetime observed corresponding to the ground state was $\tau_{exp} = 165$ ps (see Fig. 3). The first tens of picoseconds of these two signals are shown together with their Fourier transform in Fig. 4. The excited state vibrational modulation (307 fs oscillations, 109 cm^{-1}) is observed for $\tau_{12} = 460$ fs, while the ground state vibrational modulation (160 fs oscillations, 208 cm^{-1}) is observed for $\tau_{12} = 614$ fs [14,15,23]. These vibrational frequencies correspond to wave packet motion in the B state with $v' \approx 7$–10 and the X ground electronic state with $v'' \approx 3$–4, respectively [24]. The initial wave packet dephasing (dashed line) in Fig. 4a,b was obtained by eliminating the slow modulation caused by rotational dephasing and then fitting the vibrational modulation amplitude to an exponential. The data in Fig. 4a show a vibrational revival at 10 ps that is very similar to that observed in pump–probe measurements with a similar preparation pulse [25]. Because no coherence is lost during wave packet spreading, revivals are typically expected. The wave packet spreading time depends on intramolecular parameters such as anharmonicity and external parameters of the preparation pulse such as pulse duration and chirp. The value measured for wave packet spreading in the B state of 4 ps is consistent with other femtosecond pump–probe measurements [9,10]. The time associated with wave packet spreading of the X state of ~10 ps is longer indicating a much smaller anharmonicity and a smaller number of vibrational levels involved [26,27]. Our measurements on wave packet spreading are in agreement with the FWM experiments on gaseous iodine from other groups [28–30].

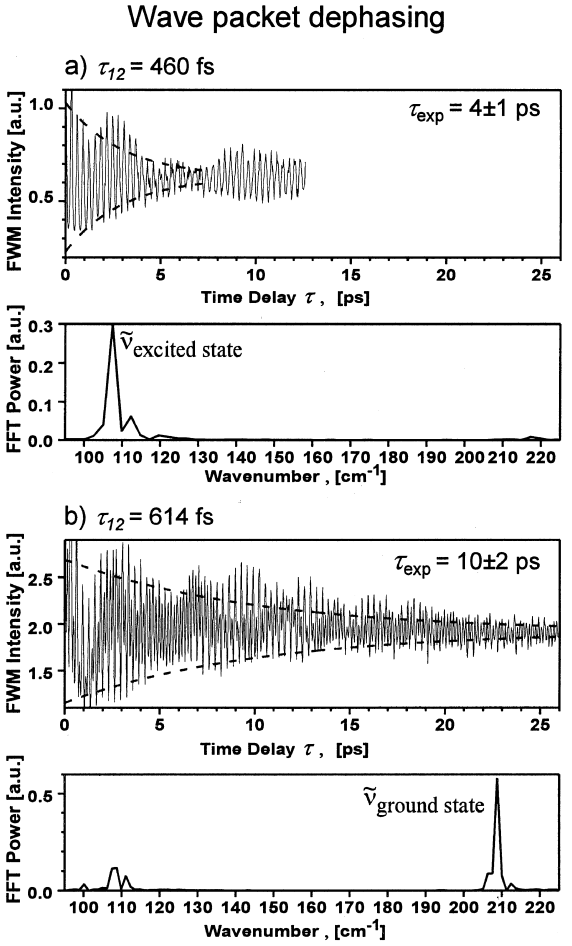

Fig. 4. Measurements of vibrational wave packet spreading in (a) excited state (only the first 12 ps) and (b) ground state with the VE pulse sequences as in Fig. 3. The decay in modulation amplitude caused by wave packet spreading was fit to an exponential function and is included here (dashed lines). The data in (a) show a wave packet revival at 10 ps. The corresponding power FFT is shown.

This Letter reports on the use of different three-pulse FWM sequences that can be effectively used to measure different types of coherence relaxation processes in gas phase molecules. From our results, we conclude that the vibronic coherence relaxation times in iodine vapor are strongly influenced by inhomogeneous broadening. We obtained the homogeneous relaxation time and the corresponding cross-section using PE measurements. The size of the cross-section indicates that decoherence is caused by long-range 'soft' collisions. In addition, we measured the inhomogeneous vibronic coherence relaxation and vibrational relaxation times following selective coherent excitation in the ground or in the excited state. Times for wave packet spreading in each state are also reported. Using different pulse sequences to select among the relaxation processes, these powerful methods can measure T_1 times (typically 10^{-8} s); T_2 times (typically 10^{-10} s) and T_3 times (typically 10^{-12} s). Future applications will explore decoherence processes in polyatomic molecules, an aspect that is of great interest for efforts in coherent control of molecular dynamics [31]. Of particular interest will be to explore the long-range dephasing collisions and the wave packet spreading rates in multi-dimensional systems.

Acknowledgements

We thank Ronnie Kosloff for his insightful comments and his presentation at the MSU on quantum dissipation. We also thank the referee of this manuscript for a thorough and insightful review. This research was funded by the National Science Foundation. I.P. gratefully acknowledges a James L. Dye Endowment Fellowship. M.D. is a Lucille and David Packard Science and Engineering Fellow, a Camille Dreyfus Teacher–Scholar, and an Alfred P. Sloan Fellow.

References

[1] N.A. Kurnit, I.D. Abella, S.R. Hartmann, Phys. Rev. Lett. 13 (1964) 567.
[2] C.K.N. Patel, R.E. Slusher, Phys. Rev. Lett. 20 (1968) 1087.
[3] E.L. Hahn, Phys. Rev. 80 (1950) 580.
[4] G.R. Fleming, M.H. Cho, Annu. Rev. Phys. Chem. 47 (1996) 109.
[5] W.P. de Boeij, M.S. Pshenichnikov, D.A. Wiersma, Annu. Rev. Phys. Chem. 49 (1998) 99.
[6] T.H. Joo, A.C. Albrecht, Chem. Phys. 173 (1993) 17.
[7] G.A. Capelle, H.P. Brodia, J. Chem. Phys 58 (1973) 4212.
[8] J.A. Paisner, R. Wallenstein, J. Chem. Phys. 61 (1974) 4317.
[9] A.H. Zewail, M. Dantus, R.M. Bowman, A. Mokhtari, J. Photochem. Photobiol. A 62 (1992) 301.

[10] C. Lienau, A.H. Zewail, J. Chem. Phys. 100 (1996) 18629.
[11] A.H. Zewail, T.E. Orlowski, K.E. Jones, D.E. Godar, Chem. Phys. Lett. 48 (1977) 256.
[12] R.W. Boyd, Nonlinear Optics, Academic Press, San Diego, 1992.
[13] S. Mukamel, Principles of Nonlinear Optical Spectroscopy, Oxford University Press, New York, 1995.
[14] I. Pastirk, E.J. Brown, B.I. Grimberg, V.V. Lozovoy, M. Dantus, Faraday Discuss. Chem. Soc. 113 (1999) 401.
[15] V.V. Lozovoy, I. Pastirk, E.J. Brown, B.I. Grimberg, M. Dantus, Int. Rev. Phys. Chem. 19 (2000) 531.
[16] E.J. Brown, Q. Zhang, M. Dantus, J. Chem. Phys. 110 (1999) 5772.
[17] E.J. Brown, I. Pastirk, B.I. Grimberg, V.V. Lozovoy, M. Dantus, J. Chem. Phys. 111 (1999) 3779.
[18] Y. Prior, Appl. Opt. 19 (1980) 1741.
[19] J.A. Shirley, R.J. Hall, A.C. Eckbreth, Opt. Lett. 5 (1980) 380.
[20] J. Tellinghuisen, J. Chem. Phys. 76 (1982) 4736.
[21] Q. Liu, C. Wan, A.H. Zewail, J. Phys. Chem. 100 (1996) 18666.
[22] A.E. Siegman, Lasers, University Science Books, Mill Valley, 1986.
[23] I. Pastirk, V.V. Lozovoy, B.I. Grimberg, E.J. Brown, M. Dantus, J. Phys. Chem. A 103 (1999) 10226.
[24] S. Gerstenkorn, P. Luc, J. Phys. 46 (1985) 867.
[25] M. Dantus, R.M. Bowman, A.H. Zewail, Nature 343 (1990) 737.
[26] M. Gruebele, A.H. Zewail, J. Chem. Phys. 98 (1993) 883.
[27] S.I. Vetchinkin, A.S. Vetchinkin, V.V. Eryomin, I.M. Umanskii, Chem. Phys. Lett. 215 (1993) 11.
[28] G. Knopp, I. Pinkas, Y. Prior, J. Raman Spectrosc. 31 (2000) 51.
[29] A. Materny, T. Chen, M. Schmitt, T. Siebert, A. Vierheilig, V. Engel, W. Kiefer, Appl. Phys. B 71 (2000) 299.
[30] R. Zadoyan, V.A. Apkarian, Chem. Phys. Lett. 326 (2000) 1.
[31] R.J. Gordon, S.A. Rice, Annu. Rev. Phys. Chem. 48 (1997) 601.